

Case Report

# A Comprehensive Method of Calculating Maximum Bridge Scour Depth

Rupayan Saha <sup>1</sup>, Seung Oh Lee <sup>2</sup> and Seung Ho Hong <sup>1,\*</sup>

<sup>1</sup> Department of Civil and Environmental Engineering, West Virginia University, 1306 Evansdale Drive, Morgantown, WV 26506, USA; rs0002@mix.wvu.edu

<sup>2</sup> Department of Civil Engineering, Hongik University, 94 Wausan-ro, Mapo-gu, Seoul 04066, Korea; seungho.lee@hongik.ac.kr

\* Correspondence: sehong@mail.wvu.edu; Tel.: +1-304-293-9926

Received: 4 October 2018; Accepted: 1 November 2018; Published: 3 November 2018



**Abstract:** Recently, the issues of scour around a bridge have become prominent because of the recurrent occurrence of extreme weather events. Thus, a bridge must be designed with the appropriate protection measures to prevent failure due to scour for the high flows to which it may be subjected during such extreme weather events. However, the current scour depth estimation by several recommended equations shows inaccurate results in high flow. One possible reason is that the current scour equations are based on experiments using free-surface flow even though extreme flood events can cause bridge overtopping flow in combination with submerged orifice flow. Another possible reason is that the current practice for the maximum scour depth ignores the interaction between different types of scour, local and contraction scour, when in fact these processes occur simultaneously. In this paper, laboratory experiments were carried out in a compound shape channel using a scaled down bridge model under different flow conditions (free, submerged orifice, and overtopping flow). Based on the findings from laboratory experiments coupled with widely used empirical scour estimation methods, a comprehensive way of predicting maximum scour depth is suggested which overcomes the problem regarding separate estimation of different scour depths and the interaction of different scour components. Furthermore, the effect of the existence of a pier bent (located close to the abutment) on the maximum scour depth was also investigated during the analysis. The results show that the location of maximum scour depth is independent of the presence of the pier bent but the amount of the maximum scour depth is relatively higher due to the discharge redistribution when the pier bent is absent rather than present.

**Keywords:** bridge scour; sediment transport; submerged flow; physical hydraulic modeling

## 1. Introduction

When a bridge is constructed in a river, the flow pattern around the bridge changes because a unique flow field develops locally around the bridge pier and abutment. Furthermore, reduced flow area through the bridge opening by the existence of embankment/abutments at both and/or one side of the river results in higher flow velocity due to the acceleration. This unique flow field with the higher velocity can seriously damage bridge foundations. Thus, if the depth of the foundation is not deep enough, the chance of bridge failure becomes higher.

A bridge can fail because of several causes, such as earthquake, wind, and flooding. Among them, bridge scour is the biggest reason of bridge failure [1,2]. For example, about 60% of bridge failures of total bridge collapse in the United States since 1950 have been related to the scour of bridge foundations [3]. The Colorado Department of Transportation (CDOT) estimated a minimum of 30 state highway bridges were destroyed and twenty were seriously damaged by floods in the year of 2013 [4].

In Nepal, due to the degradation of bed materials during the 2014 flooding, the foundation of the highway bridge over the Tinau River was seriously exposed [5]. As explained in the above examples, it is justified to say that bridge scour is one of the main bridge safety problems all over the world. Thus, accurate prediction of scour at the bridge foundation becomes the primary aim of engineers for the safety of a bridge.

Since the late 1950s, numerous studies on scour around bridges have been conducted and have generated formulas for equilibrium scour depth estimation at bridge foundations [6–9]. Although using equilibrium scour depth around a bridge foundation is a reasonable practice to design a bridge, sometimes it shows an overly conservative design compared to the field measurements. Contrary to the conservative design, a study in South Carolina found that the observed scour depth was greater than the equilibrium scour depth based on using 100-year flooding even if there had not been a 100-year flooding since the bridge was built [10,11]. Repeated occurrences of smaller flooding events might cause scour that was greater than the scour estimation in South Carolina. Moreover, some researchers have used computational fluid dynamics (CFD) simulations and found that the scour depth was under-predicted by the steady-state calculations while it was over-predicted by the unsteady-state [12,13].

One of the possible reasons of lacking an accurate scour prediction method is that many of the scour predictor equations were derived from simplified laboratory studies under free flow cases. The extreme amount of water associated with huge flood events can result in a complex flow field around the bridge under bridge overtopping flow in combination with submerged orifice flow. In addition to the complex flow field, the irregular shape of river geometry as well as non-uniform sediment distribution cannot be reproduced in a simplified-idealized laboratory setting such as in rectangular flume as in the previous research. Also, most of the scour predicting equations are 2nd or 3rd order which may not accurately predict scour depth as the scouring process is a complicated scholastic phenomenon.

Another possible reason for the inaccurate prediction of scour depth is that the current practice of total scour depth assumes that contraction and local scour are independent processes. Contraction scour is the consequence of flow acceleration due to contraction in the flow area, while local scour is caused by local vortex structures around the base of the obstruction. However, when the bridges are constructed in the river, these two-flow patterns tend to occur concurrently, which make local scour and contraction scour time dependent [14]. Thus, to predict maximum scour depth around a bridge foundation, a single equation should be developed rather than two separate equations for different types of scour.

Hence, the main objective of this study is to develop a single equation that can be used to predict maximum scour depth where different types of scour occur simultaneously. A scale down laboratory experiment was conducted to find the interaction between different scour components and the result was applied to and compared with the most widely used scour equations in the US (Colorado State University (CSU) and Melville-Sheppard (M/S) equations) to suggest an improved way of calculating the maximum scour depth. These equations predict maximum pier scour depths. Basic applications include simple pier substructure configurations and riverine flow situations in alluvial sand-bed channels. The CSU equation has been used for bridge scour evaluations and bridge design for countless bridges in the U.S. and worldwide. The M/S equation combines pier geometry, shape, and angle of attack to compute an effective pier width,  $a^*$ , and also distinguishes between clear-water and live-bed flow conditions.

## 2. Materials and Methods

### 2.1. Physical River Modeling

As shown in Figure 1, a 1:60 scale down physical model was constructed in the hydraulics laboratory including full river bathymetry of the Towaliga River bridge at Macon, Georgia by using

Froude number similarities between the model and the prototype [15–17]. A relatively small bridge was selected in this experiment because a large number of smaller bridges can fail during extreme hydrologic events. The drainage area of the selected site at the bridge is 816 km<sup>2</sup>. Discharge was estimated as 1700 m<sup>3</sup>/s by the U.S. Geological Survey for Tropical Storm Alberto in 1994 which is larger than 500 year flooding. During this historic event, severe overtopping of the bridge and significant scour around the pier bents in the left floodplain occurred, but the embankment and bridge remained sufficiently intact until repairs could be made to the scoured area. The actual scour depth measured during the storm events can be found in Hong and Sturm [16,17]. As shown in Figure 1, each of the pier bents consists of two in-line rectangular columns having a width of 1 m, and they were modeled inclusive of pile caps and piles. A bridge deck width of 13 m, in accordance with standard two-lane roads was also constructed in the laboratory.



**Figure 1.** Towaliga River bridge in the field and model in the laboratory.

The approach section of the bridge was 7.3 m long followed by a 6.09 m long moveable working bed section. The approach section was filled with uniform size of small gravel ( $d_{50} = 3.3$  mm) to make a fully rough turbulent approach flow. In the moveable working bed section, the full depth was filled with sand with median diameter size ( $d_{50}$ ) of 0.53 mm. The bridge model was constructed within the moveable working bed section for the scour experiment.

For selecting sediment size in the laboratory study, recently developed scour modeling methodology was applied [2,18–20]. Selecting sediment size in the laboratory was mostly related to the ratio of pier size to sediment size ( $a/d_{50}$ ). In the field, the effect of sediment size,  $d_{50}$ , has not been considered to be important to pier scour because of very large values of  $a/d_{50}$  [21]. However, in the laboratory, pier scour depth to pier size ratio ( $d_{ps}/a$ ) tends to increase with  $a/d_{50}$  up to a maximum at  $a/d_{50} \approx 25$  and seemingly becomes independent of the ratio when  $a/d_{50}$  is greater than 50 [19]. However, another researcher has suggested that  $d_{ps}/a$  may decrease at very large values of  $a/d_{50}$  based on experiments in a large flume [22]. Therefore, the sediment size,  $d_{50}$ , was chosen such that the ratio of pier size to sediment size,  $a/d_{50}$  was in the range of 25–50 where it has negligible influence on pier scour. Furthermore, the ratio of the approach velocity to the critical velocity which concludes the condition of clear water scour regime was also an important factor to choose sediment size in the experiment. Considering all the above conditions, the sediment size for this experiment was chosen as  $d_{50} = 0.53$  mm with  $\sigma_g = 1.2$ , where  $\sigma_g$  is geometric standard deviation of the particle size distribution.

Within the working moveable bed section, the erodible embankment/abutment was constructed at both sides of the channels by using erodible fill with rock-riprap protection in order to reproduce the same conditions as in the field [16,23]. Furthermore, the existing roadway and bridge deck were modeled based on the scale-ratio and put on top of the embankments. With this approach, submerged orifice flow with and without overtopping during the extreme amount of flooding as observed in the field could be simulated in the laboratory. As shown in Figure 2, eight pier bents were also constructed

through the bridge to support the bridge deck and for the local scour experiment. Each of the piers consisted of two in-line rectangular columns. Abutment structures were constructed and buried at both sides of the erodible embankments.

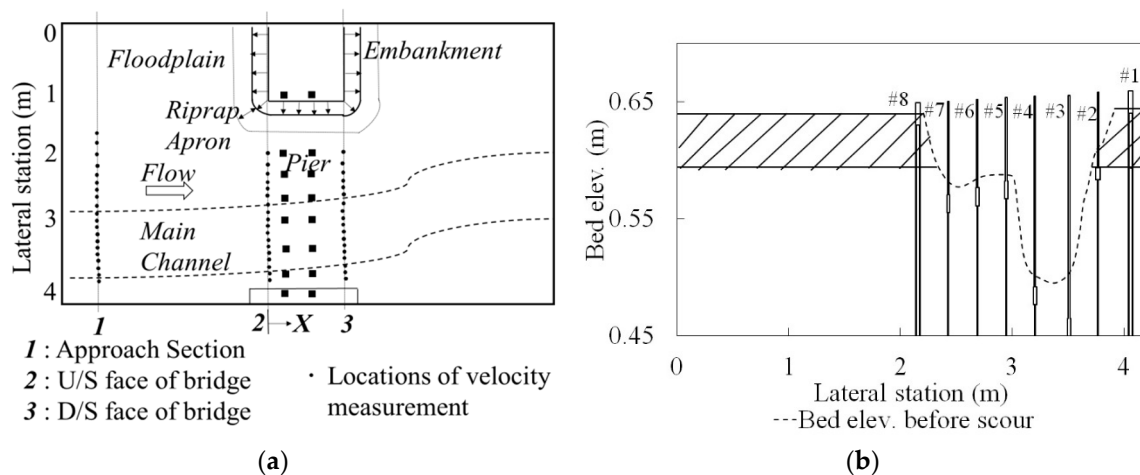


**Figure 2.** Geometry of compound channel for (a) plan view with velocity measurement locations; (b) cross section view at bridge.

## 2.2. Experimental Procedure

After completion of the model structure, the flume was slowly filled with water from a downstream supply hose to saturate the sand without disturbing the initial bottom contours. Then bottom elevations were measured in detail throughout the entire working section using an Acoustic Doppler Velocimeter (ADV). After that, a larger flow depth than the required value was set by the tailgate, then discharge was increased slowly to prevent initial scour while setting up the test discharge. Then the tailgate was lowered to achieve the desired depth of flow. In the meantime, a point gauge was used to measure the flow depth to measure the targeted water depth. Once the desired flow rate and water depth were achieved, scouring was continued for 5 to 6 days until equilibrium (change in scour depth less than 2% within 24 h) was reached. After reaching equilibrium condition, the entire bed elevation (bed elev.) was measured by a point gauge and the ADV in detail to obtain accurate contours after scour. After finishing the moveable bed experiment, the surface of the movable bed was fixed by spraying polyurethane. In the fixed bed conditions, the velocities were measured by ADV in the approach section and bridge upstream (U/S) and downstream (D/S) section. During the velocity measurements, typical correlation values in the experiments were greater than 90% and the Signal Noise Ratio (SNR) was greater than 15. The sampling frequency of the ADV was chosen to be 25 Hz with a sampling duration of 2 min at each measuring location. More detailed measurements techniques using ADV can be found in several other articles [24–29].

## 2.3. Assessment of Reference Scour Depth

Two well established theoretical pier scour equations were used to decide the reference scour depth at the pier for this research. One of the most commonly used pier scour equation in the United State is the CSU equation (also known as the HEC-18 equation). The CSU equation includes a correction factor for pier shape, angle of attack of flow, and the bed conditions. The CSU equation was initially developed from a laboratory data set measured by several researchers [6,30,31]. After the initial development, the CSU equation has been progressively modified over the years and is currently

recommended by the Federal Highway Administration (FHWA) for estimating equilibrium scour depths at simple piers as follow [6]:

$$\frac{d_{csu}}{Y_2} = 2K_1K_2K_3 \left( \frac{a}{Y_2} \right)^{0.65} Fr_2^{0.43} \quad (1)$$

where,  $K_1$ ,  $K_2$ ,  $K_3$  are the correction factors for pier nose shapers, for angle of attack of flow, and for bed conditions, respectively;  $Fr_2 = \text{Froude number at the pier face} = V_2 / (gY_2)^{0.5}$ ;  $a = \text{Pier width}$ ;  $d_{csu} = \text{Equilibrium pier scour depth}$ ;  $Y_2 = \text{Flow depth directly upstream of the pier}$ ;  $V_2 = \text{Mean velocity of flow directly upstream of the pier}$ ;  $g = \text{Acceleration of gravity}$ . Several evaluations of the CSU equation through laboratory and field datasets have shown this equation may perform better than other bridge predictive equations [32–34]

Another commonly used pier scour prediction method is the Melville–Sheppard or M/S equation [6,34,35]. A new variable is introduced in the M/S equation, effective pier width,  $a^*$ , which shows the combined effect of pier geometry, shape, and angle of attack. The equation is as follows:

$$\frac{d_{ms}}{a^*} = 2.5f_1f_2f_3 \quad (2)$$

where,  $f_1, f_2, f_3$  are the factors for flow-structure interactions, for flow-sediment interactions, and for sediment-structure interactions, respectively. Here,

$$f_1 = \tanh \left[ \left( \frac{Y_2}{a^*} \right)^{0.4} \right] \quad (3)$$

$$f_2 = \left[ 1 - 1.2 \left[ \ln \left( \frac{V_2}{V_c} \right) \right]^2 \right] \quad (4)$$

$$f_3 = \left[ \frac{\left( \frac{a^*}{d_{50}} \right)^{1.13}}{10.6 + 0.4 \left( \frac{a^*}{d_{50}} \right)^{1.33}} \right] \quad (5)$$

where,  $V_c$  is the critical velocity for movement of  $d_{50}$ , calculated by Keulegan's equation.

Using the provided theoretical pier scour equation, pier scour depth was predicted with the variables measured in the experiments. Because theoretical equations were derived from a simple laboratory set-up in a rectangular flume, the result can be used as a reference pier scour depth without any effect of flow contraction. Then, the reference pier scour depth was compared with the measured maximum scour depth around the pier where the flow contraction and local vortex structure interact and lead to the maximum scour depth. The results showed the effect of flow contraction on the pier scour and were used to suggest precise estimation of pier scour depth [8].

### 3. Results and Discussion

A total of eight experiments were conducted for this research and the experimental conditions are summarized in Table 1 where  $Q$  is the total discharge and  $q_2/q_1$  is the discharge contraction ratio which can be used as a key-independent variable that accounts for flow redistribution and resulting flow acceleration through a bridge section.  $V_1$ ,  $Y_1$ , and  $V_2$ ,  $Y_2$  are cross-sectional mean velocity, and depth of floodplain in the approach and at the upstream face of the bridge section, respectively. Also, maximum scour depth expressed as flow depth measured at the location of maximum scour ( $Y_m$ ) and longitudinal (flow direction) distance measured from the upstream face of the bridge to the location of maximum scour depth ( $X$ ) (see in Figure 2a) are presented in Table 1. A better idea of the scour distribution at the bridge cross section in these experiments can be seen in Figure 6 as a reference. Run 9 and 10 were selected from the previous study [25] and used to validate the results in this research so that

the suggested method can be used for different hydraulic and geometry conditions. As shown in Table 1, runs 1, 4, 5, and 6 were performed in free (F) flow condition; whereas, the remaining runs were conducted in the submerged flow conditions with overtopping (OT) and without overtopping (SO).

Close to the toe of the abutment where the abutment side slope ends and the first pier is introduced, these locations are the most vulnerable to scour because abutment scour, pier scour, and contraction scour occur simultaneously. Thus, to find the effect of pier on the maximum scour depth, pier bent #7 was removed from the river model and experiments were conducted in runs 7 and 8 with the exact same flow conditions as in runs 2 and 3. Even if the velocities and scour depths were measured in the entire working moveable bed section, only the floodplain flow variables and scour depths are presented in this paper because the maximum scour depth occurred on the floodplain in all our cases.

For the velocity measurements at each cross-section, point velocities were measured along multiple vertical transects through the entire cross-section, and at each vertical transect. Point velocities were measured at minimum of four points and maximum ten points vertically depending on the depth of water. Then, the depth-averaged velocity was determined by the best fit of the logarithmic velocity profile in each vertical transect. Based on the depth-averaged velocity, the cross-sectional mean velocity of the floodplain was calculated for the approach and bridge section as presented in Table 1.

**Table 1.** Experimental conditions and location of maximum scour depth measurement.

Run	Flow Type	Q (m <sup>3</sup> /s)	q <sub>2</sub> /q <sub>1</sub>	V <sub>1</sub> (m/s)	Y <sub>1</sub> (m)	V <sub>2</sub> (m/s)	Y <sub>2</sub> (m)	X (m)	Y <sub>m</sub> (m)
1	F	0.029	1.45	0.082	0.125	0.134	0.110	0.122	0.174
2	SO	0.038	1.53	0.082	0.122	0.177	0.088	0.094	0.201
3	OT	0.053	1.37	0.076	0.149	0.183	0.088	0.076	0.219
4	F	0.046	1.46	0.085	0.146	0.140	0.131	0.049	0.207
5	F	0.053	1.71	0.076	0.149	0.146	0.137	0.049	0.210
6	F	0.038	1.58	0.082	0.122	0.146	0.110	0.049	0.186
7	SO	0.038	1.53	0.082	0.122	0.177	0.088	0.186	0.202
8	OT	0.053	1.37	0.076	0.149	0.183	0.088	0.094	0.229
9	F	0.105	1.71	0.165	0.073	0.302	0.070	-	0.180
10	OT	0.198	1.05	0.219	0.149	0.390	0.088	-	0.274

Notes: F = free flow, SO = Submerged orifice flow, OT = Overtopping.

### 3.1. Measurement of the Maximum Scour Depths

Initial bottom elevations were measured throughout the test (moveable bed) section before the experiment and then the final bottom elevations were measured at the same locations in equilibrium conditions. Then, to find the location and magnitude of the maximum scour depth, bed elevations after and before the scouring were compared. The maximum scour depth in all of the laboratory experimental runs was found within the bridge and close to the bridge pier (Table 1).

### 3.2. Prediction of Maximum Scour Depth

The main assumption in this research is that maximum scour depth consists of theoretical pier scour depth and additional scour due to flow contraction. Based on this assumption, the maximum scour depth can be calculated by the equation,

$$\text{Max. Scour depth} = \text{Theoretical pier scour} + \text{Additional scour by flow contraction} \quad (6)$$

The schematic diagram is given in Figure 3 to define the variables used for the analysis. The theoretical pier scour depth can be decided using the CSU ( $d_{csu}$ ) or M/S equation ( $d_{ms}$ ) with measured flow variables and the results are shown in Table 2. Then, the “Additional scour by flow

contraction” can be determined by measured the water depth at the deepest point and theoretical pier scour depth as follows;

$$Y_{m-csu} = Y_m - d_{csu} \tag{7}$$

$$Y_{m-ms} = Y_m - d_{ms} \tag{8}$$

where,  $Y_{m-csu}$  and  $Y_{m-ms}$  are the calculated water depths at the deepest location subtracted from the total water depth at the point by the theoretical pier scour depth of CSU ( $d_{csu}$ ) or M/S equation ( $d_{ms}$ ) respectively, which stands for the resulting water depth due to the additional scour. The variables required for calculation of the reference pier scour depth using the CSU and M/S equations are listed in Tables 1 and 2. Here,  $\theta$  is the flow angle of attack at the pier face which is required to estimate correction factor,  $K_2$  and effective pier width,  $a^*$  for the CSU and M/S equations, respectively. The additional scour components are also shown in Table 2 in terms of non-dimensional variables.

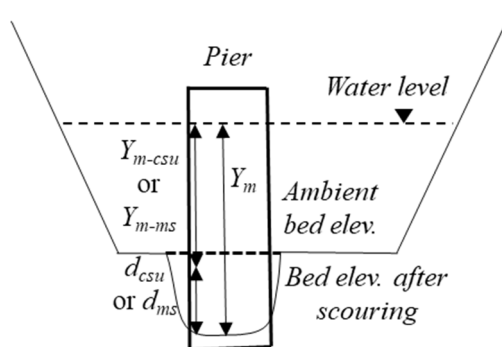


Figure 3. Schematic diagram for calculation of maximum scour depth.

Table 2. Summary of experimental results to calculate maximum scour depth.

Run	$Fr_2$	$\theta$	$a^*$ (m)	$V_2/V_c$	$d_{csu}$ (m)	$d_{ms}$ (m)	$\frac{Y_{m-ms}}{Y_1}$	$\frac{Y_{m-csu}}{Y_1}$
1	0.13	20	0.009	0.46	0.029	0.006	1.34	1.15
2	0.19	12	0.009	0.63	0.027	0.014	1.51	1.41
3	0.20	8	0.008	0.64	0.024	0.014	1.36	1.29
4	0.12	15	0.009	0.46	0.027	0.006	1.38	1.23
5	0.13	15	0.009	0.49	0.028	0.007	1.35	1.21
6	0.14	22	0.009	0.50	0.031	0.009	1.44	1.27
7	0.19	12	0.009	0.63	0.027	0.014	1.51	1.41
8	0.20	8	0.008	0.64	0.024	0.014	1.42	1.35
9	0.36	15	0.045	0.66	0.083	0.075	1.40	1.30
10	0.42	15	0.045	0.68	0.095	0.081	1.29	1.19

If the assumption is correct, the effect of additional scour due to flow contraction can be represented by the values of  $Y_{m-csu}$  and  $Y_{m-ms}$ . Thus, the non-dimensional value of additional scour components calculated using the CSU and M/S equation are compared with the measured discharge contraction ratio in Figure 4a,b respectively. As the value of flow contraction ratio increases, the normalized value of additional scour depth gradually increases. The results clearly reveal that the effect of flow contraction on the additional scour term becomes higher as the value of  $q_2/q_1$  increases. Runs 9 and 10 were also plotted in Figure 4 to validate the findings in different hydraulic and geometry conditions and the result favors the validation as it shows a similar trend of runs 9 and 10 with pressure and free flow data respectively. For both cases using the CSU equation and M/S equation, the pressure flow line has a steeper slope than for the free flow cases and lies above. Because of the vertical flow contraction in addition to the existing lateral flow contraction in pressure flow, the resulting additional scour depth due to the flow contraction is higher than in the free flow cases. Currently, additional experiments are being conducted. With more experimental conditions as well as the data set in Figure 4,

the best fit equation will be provided for calculation of scour due to flow contraction under free and pressure flow by a least square regression analysis

It is interesting to note that, the regression analysis results using only with the data set in Figure 4 show higher values of exponents of  $q_2/q_1$  in the case with the M/S pier scour equation for both of the pressure and free flow cases. This finding illustrates that the M/S equation shows a smaller value of pier scour depth in the same flow conditions compared to the CSU equation. The ratios between the theoretical pier scour depths calculated using CSU ( $d_{csu}$ ) and M/S ( $d_{ms}$ ) are plotted with the value of flow intensity factor ( $V_2/V_c$ ) in Figure 5. As shown in Figure 5, the M/S equation shows almost 50% to 75% underestimated values compared to the CSU results. The CSU pier scour equation was developed for live-bed scour and thus ignores the effect of different values of flow intensity and assumes the value is equal to 1; but in the M/S equation,  $V_2/V_c$  is considered as an individual factor to account for the effect of clear water conditions and varies from 0.3 to 1. So, it is obvious that the CSU pier scour equation shows a larger value when applied to the clear water condition. However, there is another important difference between the CSU and M/S equations, which is the consideration of bed material size. However, in our case, the effect of sediment size cannot be considered because all of the experiments are conducted with same sediment size.

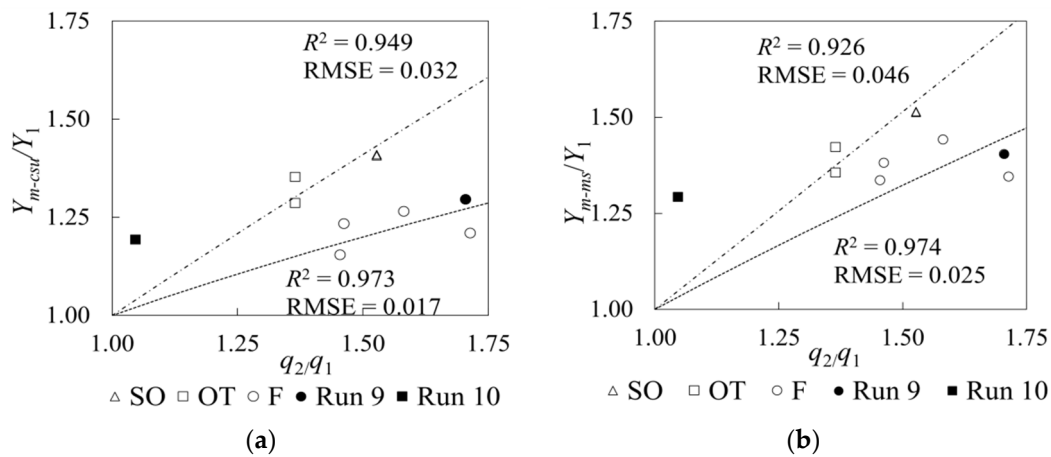


Figure 4. Effect of flow contraction on additional scour components using (a) Colorado State University (CSU) and (b) Melville-Sheppard (M/S) equations.

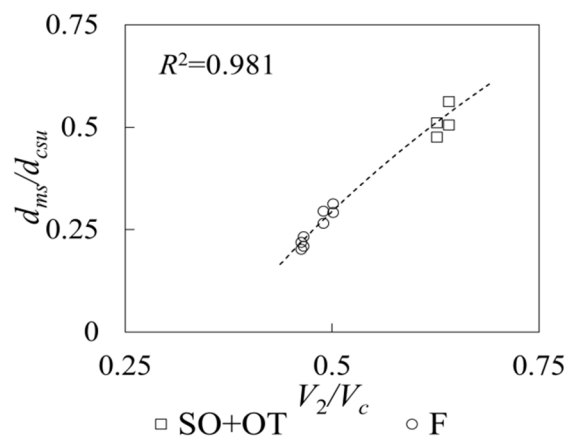
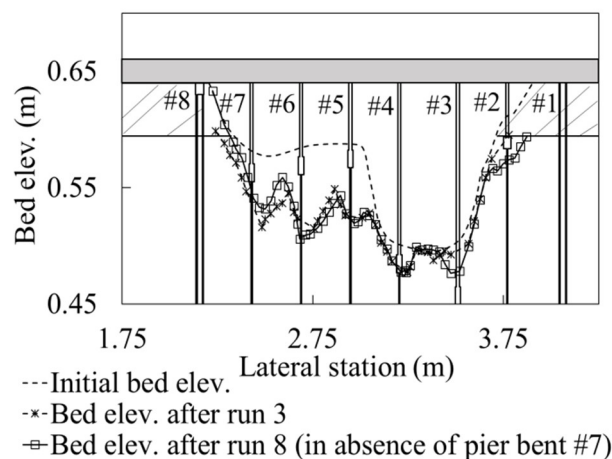


Figure 5. Comparison of CSU and M/S pier scour depth in terms of flow intensity.

Finally, a comprehensive procedure for predicting the maximum scour depth with respect to bridge design is introduced:

1. Collecting field geometry data including sediment size;
2. Calculate the flow variables using software or hydraulic laboratory modeling;
3. Compute the theoretical pier scour depth from established pier scour equations (CSU or M/S equations);
4. The additional scour depth due to the effect of flow contraction can be estimated with the equations developed by regression analysis with the data in Figure 4 as well as more laboratory/field data sets;
5. Adding the results from steps 3 and 4 to predict the maximum scour depth for bridge design.

In addition to suggest a comprehensive procedure, the effect of pier bent (located near to the abutment) on maximum scour depth was investigated qualitatively. As shown in Table 1, runs 7 and 8 were conducted with the exact same flow condition as in runs 2 and 3 respectively, but removing pier bent #7 in the bridge section. Figure 6 shows the cross-section comparisons between runs 3 and 8 after scouring. The maximum scour depth occurred at pier bent #6 for both runs 3 and 8. So, the location was independent of the presence of the closest pier bent (#7). However, the amount of maximum scour depth was slightly higher in the case of run 8 where pier bent #7 was absent. A similar trend was observed for runs 2 and 8. Discharge redistribution over the time and interaction between each pier can be the result for this difference of maximum scour depth and needs further study.



**Figure 6.** Comparison of cross-sections for runs 3 and 8.

#### 4. Conclusions

Many investigations have been made attempting to estimate the maximum scour depth and to understand the mechanism of scour around bridge piers. Most of the previous investigations were based on lab experiments using a rectangular channel under free flow. However, due to the recent extreme rainfall events, submerged orifice flow and overtopping flow occur at the bridge frequently, where the flow field around the bridge substructure is more complex than in free flow because of vertical flow contraction in addition to existing lateral flow contraction. Furthermore, most of the natural channel shapes are not rectangular. Also, the current guidelines recommended by HEC-18 assumed that contraction and local scour processes are independent and so they can be determined separately and summed to estimate total scour depth. However, during large flooding events, local scour and contraction scour occur simultaneously and a separate calculation of local scour and contraction scour results in inaccurate scour depth. To overcome the weak points that the current methodology has, laboratory experiments were carried out in a scaled down physical model and a single equation was developed to predict maximum scour depth which can be used without separate calculation of different types of scour components in pressure flow as well as in free flow cases.

Based on the basic assumption of maximum scour depth as summation of theoretical pier scour depth and additional scour depth due to flow contraction, a comprehensive way of predicting maximum scour depth in clear water conditions was suggested. Furthermore, the results demonstrate that the contraction effect on maximum scour depth increases as the flow contraction ratio increases. Also, due to additional vertical contraction in the pressure flow case, the effect of flow contraction on the maximum scour depth shows up larger than in free flow. Another outcome from our investigation concludes that the location of the maximum scour depth is independent of the existence of the closest pier bent but the absence of the closest pier bent increases the scour depth.

Even though this study suggested an improved method for the scour depth prediction in clear water conditions, a well-designed physical model is recommended to investigate the scour characteristics under live bed conditions. In addition, different sediment sizes and non-uniform size sediment should be incorporated in the future research, as natural rivers generally consist of non-uniform sediment. Finally, scour modelling using computational fluid dynamics (CFD) should also be explored to refine the proposed equation for design purposes.

**Author Contributions:** S.H.H. and S.O.L. provided background data and motivation. S.H.H. and S.O.L. designed the experiments and determined the results; R.S. analyzed the data; R.S. and S.H.H. contributed to motivation, data analysis input, and interpretation of results; R.S. and S.H.H. interpreted the results and wrote the paper; and all authors participated in final review and editing of the paper.

**Funding:** National Research Foundation of Korea (NRF) grant funded by the Korea government (MSIT) (NRF-2017R1A2B2011990); West Virginia University internal grant.

**Acknowledgments:** The laboratory data used in this paper were measured in Georgia Tech and the permission was granted by Seung Ho Hong and Seung Oh Lee.

**Conflicts of Interest:** The authors declare no conflict of interest.

## References

1. Kattell, J.; Eriksson, M. *Bridge Scour Evaluation: Screening, Analysis, and Countermeasures*; General Technical Reports 9877 1207-SDTDC; U.S. Department of Agriculture: San Dimas, CA, USA, 1998.
2. Melville, B.W.; Coleman, S.E. *Bridge Scour*; Water Resources Publications, LLC: Highlands Ranch, CO, USA, 2000.
3. Shirhole, A.M.; Holt, R.C. *Planning for A Comprehensive Bridge Safety Program*; Transportation Research Record No. 1290; Transportation Research Board, National Research Council: Washington, DC, USA, 1991.
4. Novey, M. Cdot Assessing ‘Millions and Millions’ in Road Bridge Damage. Available online: [www.coloradoan.com](http://www.coloradoan.com) (accessed on 15 September 2013).
5. Shrestha, C.K. Bridge Pier Flow Interaction and Its Effect on the Process of Scouring. Ph.D. Thesis, University of Technology Sydney (UTS), Ultimo, Australia, 2015.
6. Arneson, L.A.; Zevenbergen, L.W.; Lagasse, P.F.; Clopper, P.E. *Evaluating Scour at Bridges*, 15th ed.; FHWA-HIF-12-003, HEC-18; Department of Transportation, Federal Highway Administration: Washington, DC, USA, 2012.
7. Lee, S.O. Physical Modeling of Local Scour Around Complex Bridge Piers. Ph.D. Thesis, School of Civil and Environmental Engineering, Georgia Institute of Technology, School of Civil and Environmental Engineering, Georgia Institute of Technology, Atlanta, GA, USA, 2006.
8. Sheppard, D.; Melville, B.; Demir, H. Evaluation of Existing Equations for Local Scour at Bridge Piers. *J. Hydraul. Eng.* **2014**, *140*, 14–23. [[CrossRef](#)]
9. Sturm, T.W.; Ettema, R.; Melville, B.M. *Evaluation of Bridge-Scour Research: Abutment and Contraction Scour Processes and Prediction*; NCHRP 24-27; National Co-operative Highway Research Program: Washington, DC, USA, 2011.
10. Melville, B.; Chiew, Y. Time Scale for Local Scour at Bridge Piers. *J. Hydraul. Eng.* **1999**, *125*, 59–65. [[CrossRef](#)]
11. Shatanawi, K.M.; Aziz, N.M.; Khan, A.A. Frequency of discharge causing abutment scour in South Carolina. *J. Hydraul. Eng.* **2008**, *134*, 1507–1512. [[CrossRef](#)]

12. Alemi, M.; Maia, R. Numerical Simulation of the Flow and Local Scour Process around Single and Complex Bridge Piers. *IJCE* **2018**, *16*, 475. [[CrossRef](#)]
13. Sajjadi, S.A.H.; Sajjadi, S.H.; Sarkardeh, H. Accuracy of numerical simulation in asymmetric compound channels. *IJCE* **2018**, *16*, 155. [[CrossRef](#)]
14. Hong, S. Interaction of Bridge Contraction Scour and Pier Scour in a Laboratory River Model. Master's Thesis, School of Civil and Environmental Engineering, Georgia Institute of Technology, Atlanta, GA, USA, 2005.
15. Hong, S.; Lee, S.O. Insight of Bridge Scour during Extreme Hydrologic Events by Laboratory Model Studies. *KSCE J. Civ. Eng.* **2017**, *22*, 1–9. [[CrossRef](#)]
16. Hong, S.; Sturm, T.W. Physical modeling of abutment scour for overtopping, submerged orifice, and free surface flows. In Proceedings of the 5th Conference on Scour and Erosion, San Francisco, CA, USA, 7–10 November 2010.
17. Hong, S.; Sturm, T.W. Physical model study of bridge abutment and contraction scour under submerged orifice flow conditions. In Proceedings of the 33rd IAHR Congress: Water Engineering for a Sustainable Environment, Vancouver, BC, Canada, 9–14 August 2009.
18. Fael, C.M.S.; Simarro-Grande, G.; Martin-Vide, J.P.; Cardoso, A.H. Local scour at vertical wall abutments under clear-water flow conditions. *Water Res. Res.* **2006**, *10*, 1–12. [[CrossRef](#)]
19. Hong, S.; Abid, I. Physical Model Study of Bridge Contraction Scour. *KSCE J. Civ. Eng.* **2016**, *20*, 2578–2585. [[CrossRef](#)]
20. Lee, S.O.; Sturm, T.W.; Gotvald, A.; Landers, M. Comparison of laboratory and field measurements of bridge pier scour. In Proceedings of the Second International Conference on SCOUR and EROSION-ICSE, Meritus Mandarin, Singapore, 14–17 November 2004; pp. 231–239.
21. Lee, S.O.; Sturm, T.W. Effect of sediment size scaling on physical modeling of bridge pier scour. *J. Hydraul. Eng.* **2009**, *135*, 793–802. [[CrossRef](#)]
22. Sheppard, D.; Odeh, M.; Glasser, T. Large Scale Clear-Water Local Pier Scour Experiments. *J. Hydraul. Eng.* **2004**, *130*, 957–963. [[CrossRef](#)]
23. Ettema, R.; Kirkil, G.; Muste, M. Similitude of large-scale turbulence in experiments on local scour at cylinders. *J. Hydraul. Eng.* **2006**, *132*, 33–40. [[CrossRef](#)]
24. Hong, S.; Sturm, T.W.; Stoesser, T. Clear Water Abutment Scour in a Compound Channel for Extreme Hydrologic Events. *J. Hydraul. Eng.* **2015**, *141*, 1–12. [[CrossRef](#)]
25. Hong, S. Prediction of Clear Water Abutment Scour Depth in Compound Channel for Extreme Hydrologic Events. Ph.D. Thesis, School of Civil and Environmental Engineering, Georgia Institute of Technology, Atlanta, GA, USA, 2011.
26. Lane, S.N.; Biron, P.M.; Bradbrook, K.F.; Butler, J.B.; Chandler, J.H.; Crowell, M.D.; McLelland, S.J.; Richards, K.S.; Roy, A.G. Three-dimensional measurement of river channel flow processes using acoustic Doppler velocimetry. *Earth Surf. Process. Landf.* **1998**, *23*, 1247–1267. [[CrossRef](#)]
27. SonTek. *Acoustic Doppler Velocimeter (ADV) Principles of Operation*; SonTek Technical Notes; SonTek: San Diego, CA, USA, 2001.
28. Wu, P.; Hirshfield, F.; Sui, J. ADV measurements of flow field around bridge abutment under ice cover. CGU HS Committee on River Ice Processes and the Environment. In Proceedings of the 17th Workshop on River Ice, Edmonton, AB, Canada, 21 July 2013.
29. Ben Meftah, M.; Mossa, M. Scour holes downstream of bed sills in low-gradient channels. *J. Hydraul. Res.* **2006**, *44*, 497–509. [[CrossRef](#)]
30. Chabert, J.; Engeldinger, P. *Etude Des Affonillements Author Des Piles Des Ponts*; Laboratoire National d'Hydraulique de Chatou: Chatou, France, 1956.
31. Shen, H.W.; Schneider, V.R.; Karaki, S. Local scour around bridge piers. *J. Hydraul. Div.* **1969**, *95*, 1919–1940.
32. Gaudio, R.; Grimaldi, C.; Tafarojnoruz, A.; Calomino, F. Comparison of formulae for the prediction of scour depth at piers. In Proceedings of the 1st IAHR European Division Congress, Edinburgh, UK, 4–6 May 2010.
33. Gaudio, R.; Tafarojnoruz, A.; Bartolo, S.D. Sensitivity analysis of bridge pier scour depth predictive formulae. *J. Hydroinform.* **2013**, *15*, 939–951. [[CrossRef](#)]

34. Ferraro, D.; Tafarojnoruz, A.; Gaudio, R.; Cardoso, A.H. Effects of pile cap thickness on the maximum scour depth at a complex pier. *J. Hydraul. Eng.* **2013**, *139*, 482–491. [[CrossRef](#)]
35. Melville, B.W. Pier and abutment scour: Integrated approach. *J. Hydraul. Eng.* **1997**, *123*, 125–136. [[CrossRef](#)]



© 2018 by the authors. Licensee MDPI, Basel, Switzerland. This article is an open access article distributed under the terms and conditions of the Creative Commons Attribution (CC BY) license (<http://creativecommons.org/licenses/by/4.0/>).